

## Thermal Induced Dynamics of Gain Competition in Yb-doped Symmetry-Free Photonic Crystal Fibers

Katia Tragni\*<sup>(1)</sup>, Carlo Molardi<sup>(1)</sup>, Federica Poli<sup>(1)</sup>, Lorenzo Rosa<sup>(2)</sup>, Annamaria Cucinotta<sup>(1)</sup>, and Stefano Selleri<sup>(1)</sup>

(1) Department of Engineering and Architecture, University of Parma, Parco Area delle Scienze 181/A, I-43124 Parma, Italy

(2) Nanotechnology Facility, Center for Micro-Photonics, Swinburne University of Technology, Victoria 3122, Australia

### Abstract

A fiber amplifier based on Yb-doped Symmetry-Free Photonic Crystal Fiber has been studied through the use of a numerical tool. The amplification properties and the modal content of the amplifier have been investigated in conditions of severe heat load, in order to understand the effectiveness of amplification dynamics. The numerical tool, used for this study, is based on a FEM modal solver combined with a model which allows to evaluate amplification and thermal effects. Results depict a scenario where it is possible to obtain a good mode discrimination and a robust amplification under critical thermal condition.

### 1. Introduction

In the modern scientific and technological context, the improvement of fiber lasers performances is, with no doubt, pushed on an upper level by the use of Yb-doped Photonic Crystal Fibers (PCFs) amplifiers [1]. Generally speaking, fiber lasers presents advantages in terms of thermal dissipation and emission quality with respect to the other laser systems based on semiconductors or gases. Moreover, the choice of Ytterbium, with its high quantum efficiency, and the possibilities offered by PCFs technology to enlarge the core area while maintaining single mode (SM) operation, have created new perspectives for the use of fiber lasers in several applications, ranging from medical treatments to precise machining [2]. Nevertheless, the request for output power scaling cannot avoid to treat with thermal effects created during the pump absorption in the amplification process. The significant heat density, generated in the core area by quantum defect, can alter the propagation properties of the fiber amplifier. In this scenario it is possible to run up against unwanted couplings between core and cladding modes, resulting in detrimental effects like mode instability, actually spoiling the output quality [3]. The use of Symmetry Free PCFs (SF-PCFs) designs, where every kind of mirror symmetry in the inner cladding is avoided, has shown an improved single mode behaviour and a good resilience to thermal effects [4-5]. In fact, a strong delocalization of Higher Order Modes (HOMs) can be achieved also under strong thermal conditions. Even if the Fundamental Mode (FM) is significantly less affected by mode delocalization, the onset of unwanted couplings between FM and cladding modes can appear, in particular in absence of thermal load. Such a drawback can

compromise the effectiveness of the amplification process, requiring, in principle, a much more accurate amplifier design with a complete understanding of thermal dynamics.

In this contribution air-silica Yb-doped, rod-type, double cladding (DC), SF-PCFs amplifier designs have been considered and numerically investigated, setting the focus on the amplification dynamics in presence of severe thermal load. In order to achieve consistent simulations, a custom-made software have been used. This tool, built on a full vector FEM modal solver, implements a model which permits to take in account both mode competition during amplification and changes of propagation properties driven by thermal load [6].

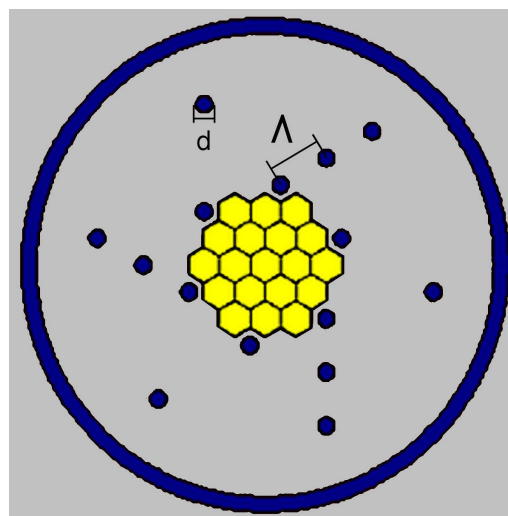


**Figure 1.** Cross-section of the double cladding SF-PCF analyzed in this contribution.

### 2. Fiber Design

The amplifier consists in a special PCF with a design directed to avoid mirror symmetries. This design aim is to improve the delocalization of HOMs whose spatial distribution suffers the lack of symmetry, i.e. mainly HOMs from  $LP_{lx}$  family, while maintaining nearly untouched the FM which benefits from circular cross section distribution. The cross section of this PCF, shown in Figure 1, is composed by a core obtained by substituting the innermost 19 cells with Yb-doped rods. The cladding is obtained surrounding the core with one

tilted ring of holes and other two rings, partially filled, characterized by a wings shape. The distance between two neighbouring cells, namely the pitch  $\Lambda$ , is equal to  $15 \mu\text{m}$  and the normalized air-hole diameter  $d/\Lambda$  is equal to 0.5. Eventually the cladding is surrounded by an air-cladding with thickness of  $7 \mu\text{m}$ . For the purpose of the study, the cladding diameter has been set to  $17\Lambda$ . The amplifier length is set equal to 1 m, and the dopant concentration is supposed to pledge a pump absorption of 27 dB/m. As the amplifier is intended to be a not flexible rod-type fiber, the cross section depicted in Figure 1 is built inside a rigid silica structure with a diameter equal to 1.5 mm.

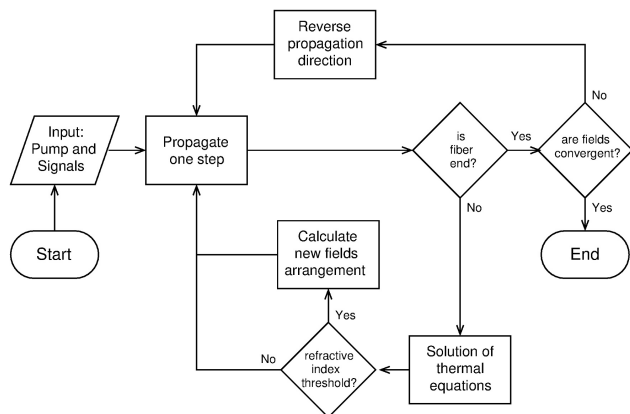


**Figure 2.** Flowchart of the simulator operations.

### 3. Numerical Analysis

The analysis has been achieved through the use of a custom made software which takes in account the propagation and the spatial gain of the modes of interest along the amplifier length. Furthermore the software has been supplied with a thermal model in order to evaluate the increase of temperature inside the fiber core and, consequently, to evaluate the changes of guidance properties along the fiber. The simulator operation moves through the following steps, as shown in the flowchart of Figure 2. At the beginning the field of the modes of interest and their overlap, defined as the normalized field intensity over the core area, are calculated using a FEM modal solver. Then, after the setting of the initial conditions of pump and signal power, pump and signal are propagated along the fiber length, namely  $z$ -direction. The fiber is divided in small steps along  $z$  and the amplification is implemented solving the population and propagation equations, considering the spatial interaction between the fields and the dopant. During the propagation a numerically efficient thermal model, which considers the fiber as a concentric structure with different layers, is used to evaluate the amount of temperature accumulated in the fiber core. The increase of temperature modifies the refractive index, according to the thermal lens effect [7], so the propagation properties of the modes are calculated again when a fixed threshold on the index variation is reached. This procedure is reiterated step by step along  $z$ , forth and back, until the fields relax on convergent values.

For the purpose of this analysis, a pump source of 400 W at 976 nm has been chosen. Co-propagating and counter-propagating pump configurations have been investigated. Regarding the input signals, only FM and the first HOM, namely  $LP_{11}$ , which is the most detrimental one for SM regime, have been taken in consideration at a wavelength of 1030 nm. The starting power for the FM and the first HOM have been set to 5 W and 50 mW, respectively. Such values are in agreement with the typical HOM excitation given by the finite alignment precision of the input signal in experimental setups [8]. In order to correctly implement the boundary condition of the thermal problem, the rod fiber has been considered cooled by air convection at a temperature of  $25^\circ\text{C}$ .

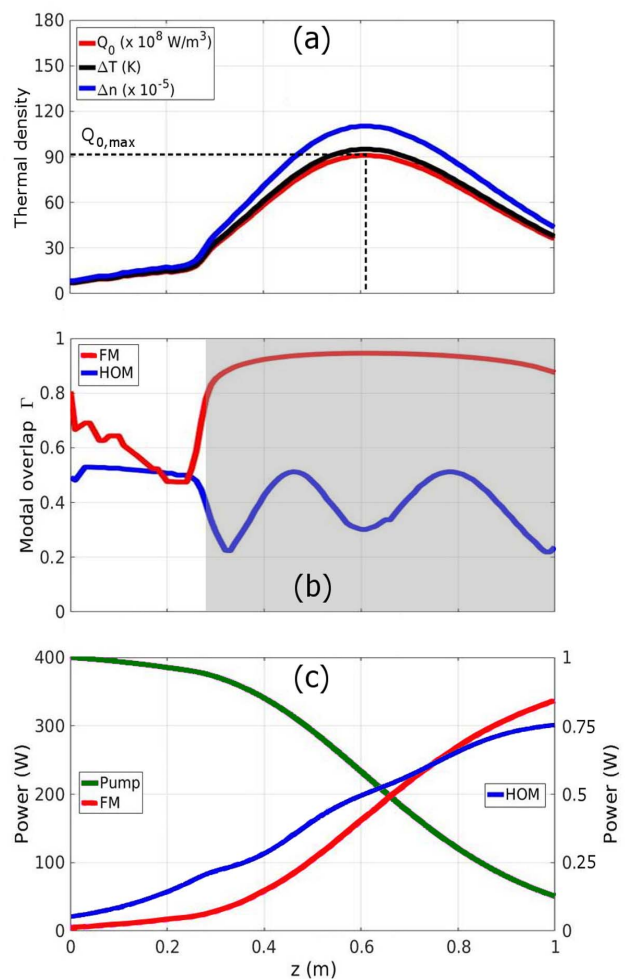


**Figure 3.** Co-propagating pump case: (a) Thermal density, temperature offset, and refractive index variation over propagation direction  $z$ ; (b) mode overlap of FM and first HOM over  $z$ ; (c) pump, FM, and first HOM power evolution over  $z$ .

### 4. Results

The first set of simulations has been performed considering the configuration with co-propagating pump. Results are shown in Figure 3(a)-(c). It is possible to

notice that in the condition of cold fiber, i.e. when the pump is partially absorbed in the first span of the fiber, roughly 25 cm long, the propagation of the FM appears to be arduous. From Figure 3(b) it is possible to see that the FM overlap starts with a value of 0.8 and decreases to a value of 0.5. Since the modes shall become more confined with the increase of the temperature and the onset of thermal lens effect, this phenomenon can be explained with an anti-crossing coupling of the FM with one of the cladding modes. After this region of instable operation, the pump is absorbed much more rapidly, reaching a maximum value of heat density  $Q_{0,max}$  of  $91 \times 10^8 \text{ W/m}^3$  at  $z$  equal to 61 cm. This fact induces the FM to become well confined in the core area, with an overlap value equal to 0.95, ensuring a good guidance and an effective amplification. After the peak of pump absorption, the pump depletion forces the temperature to decrease, however the FM confinement remains quite good with an overlap of roughly 0.9 at the fiber output. Regarding the behavior of the first HOM, it is worth noting that this mode is delocalized by the fiber structure. This fact implies a greater instability of this mode, with several evident anti-crossing with other cladding modes. The dumps and the valleys, shown in Figure 3(b), depict an alternation of  $LP_{11}$ -like modes which become sequentially more confined varying the thermal conditions of the amplifier along  $z$ . Nevertheless, the overlap of the first HOM is maintained under the value of 0.5, thanks to ability of this SF fiber design to effectively delocalize the most detrimental HOMs. The criterion of SM operation, which is usually used, says that it is obtained when the FM overlap is more than 0.8 and the overlap difference between the FM and the most detrimental HOM is greater than 0.3 [4]. According to this criterion, SM regime is reached in this amplifier at  $z$  equal to 28 cm and maintained up to the fiber output, as shown by the shaded region of Figure 3(b). The amplification behavior is shown in Figure 3(c). The FM is amplified to a power of 338 W at the fiber output, while the power of the first HOM is around 0.75 W. These values correspond to a gain of 18.3 dB and 11.8 dB, respectively for the FM and the first HOM.

The results concerning the case of counter-propagating pump are shown in Figure 4(a)-(c). The evolution of heat density and, consequently, the temperature increase are quite different with respect to the co-propagating pump case. As the pump is injected at the fiber output, when the amplified signal is expected to be stronger, the pump depletion is higher. This results in a higher heat density at the fiber end with a  $Q_{0,max}$  equal to  $162 \times 10^8 \text{ W/m}^3$ , as shown in Figure 4(a). Looking at the fiber input, the region of “cold” fiber is now extended to a length of more than 35 cm. In this situation the FM guidance becomes more critical. It is possible to see from Figure 4(b) that the FM is experiencing a large number of couplings with cladding modes, with its overlap rapidly bouncing between 0.75 and 0.50. As previously stressed, this behavior is extended up to 35 cm, thus reducing the effective length of the fiber where it is possible to achieve

an efficient amplification. Furthermore, considering the stronger pump absorption in the last section of the fiber, the thermal lens effect, induced by the higher heat density, causes not only a strong and rapid FM confinement but also an unwanted first HOM confinement.

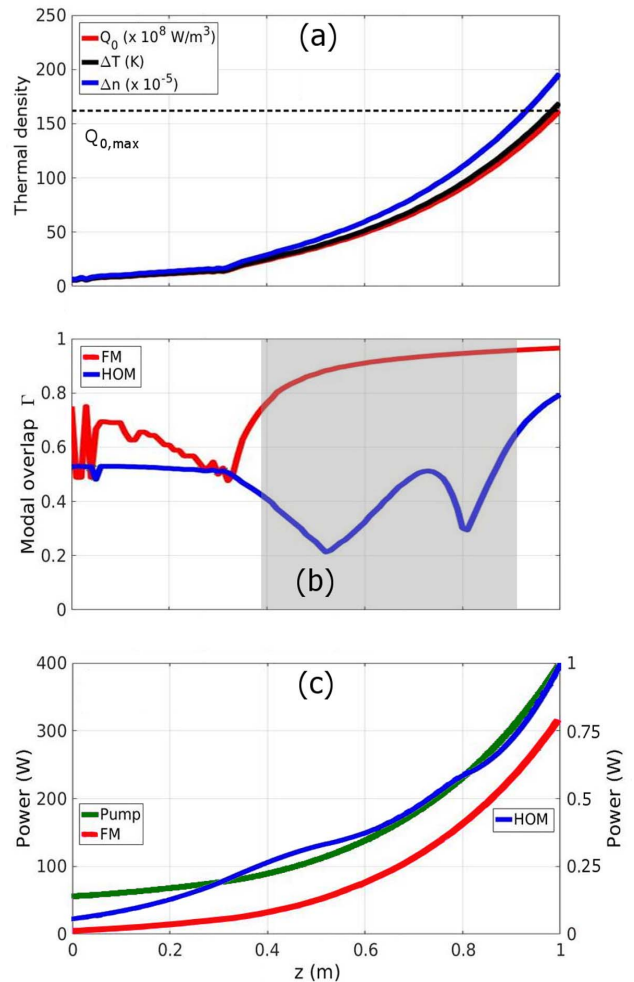


**Figure 4.** Counter-propagating pump case: (a) thermal density, temperature, and refractive index variation over propagation direction  $z$ ; (b) mode overlap of FM and first HOM over  $z$ ; (c) pump, FM, and first HOM power evolution over  $z$ .

As it is possible to see from Figure 2(b), at the fiber output the FM overlap is touching the value of 0.97 and the first HOM overlap is roughly around 0.80. Therefore, in the counter-propagating pump case the SM regime criterion is not fulfilled at the fiber output. Such an event can be detrimental for the output beam quality of the amplifier. In Figure 4(b), the region of SM operation, which is ranging from 39 cm to 91 cm, is shown with a shaded area. Regarding the amplified power, from Figure 4 (c), it is possible to see that the FM mode output power, whose value is 315 W, is less than the one obtained in the co-propagating pump case. Besides, the first HOM reaches a power of 1 W, a value which is higher with respect to the co-propagating case. In terms of gain, the FM is gaining 18 dB and the first HOM 13.1 dB. It clearly

appears that the counter-propagating pump is a worse solution than the co-propagating case, since the higher accumulation of heat is more difficult to treat, the fiber span which ensures an effective amplification is reduced, the SM operation at the fiber end is lost, and, in general, the gain competition is less efficient.

## 5. Conclusion

In this work a Yb-doped fiber amplifier based on a DC PCF with a mirror symmetry free design has been deeply analyzed with the help of a custom made numerical tool. This simulator merges FEM based modal solver with a spatial model able to evaluate amplification and mode competition along the propagation direction. Furthermore, the simulator is provided with a complete and numerically efficient thermal model, which can calculate the guidance changes induced by the increase of temperature in the core of the fiber. The amplifier under investigation has been analyzed considering forward and backward pump, with a power of 400 W, independently. As can be understood from the results, the thermal load action has a strong impact on guidance properties. In particular, it is possible to see that, in the case of “cold” fiber, the guidance of FM is quite compromised with poor mode discrimination and evidences of FM anti-crossing. The situation gets better when the amplifier starts to warm up with a clear predominance of the FM over the HOM, thus preserving SM operation and amplification effectiveness. The comparison between backward and forward pumping shows that co-propagating is a better solution, achieving a larger discrimination of the first HOM at the amplifier output.

## 6. References

1. M. N. Zervas, and C. A. Codemard, “High Power Fiber Lasers: A Review,” *IEEE J. Sel. Topics Quantum Electron.*, **20**, 5, 2014, pp. 219-241, doi: 10.1109/JSTQE.2014.2321279.
2. W. Shi, Q. Fang, X. Zhu, R. A. Norwood, and N. Peyghambarian, “Fiber lasers and their applications [Invited],” *Appl. Opt.*, **53**, 28, 2014, pp. 6554-6568, doi: 10.1364/AO.53.006554.
3. B. Ward, C. Robin, and I. Dajani, “Origin of thermal modal instabilities in large mode area fiber amplifiers,” *Opt. Express*, **20**, 10, 2012, pp. 11407-11422, doi: 10.1364/OE.20.011407.
4. E. Coscelli, C. Molardi, M. Masruri, A. Cucinotta and S. Selleri, “Thermally resilient Tm-doped large mode area photonic crystal fiber with symmetry-free cladding,” *Opt. Express*, **22**, 8, 2014, pp. 9707-9714, doi: 10.1364/OE.22.009707.
5. F. Poli, E. Coscelli, A. Cucinotta, S. Selleri and F. Salin, “Single-Mode Propagation in Yb-Doped Large Mode Area Fibers With Reduced Cladding Symmetry,” *IEEE Photon. Technol. Lett.*, **26**, 24, 2014, pp. 2454-2457, doi: 10.1109/LPT.2014.2358690.
6. L. Rosa, E. Coscelli, F. Poli, A. Cucinotta, and S. Selleri, “Full-vector modeling of thermally-driven gain competition in Yb-doped reduced symmetry photonic-crystal fiber,” *Opt. Quant. Electron.*, **48**, 3, 2016, pp. 221, doi: 10.1007/s11082-016-0493-2.
7. D. C. Brown and H. J. Hoffman, “Thermal, stress, and thermo-optic effects in high average power double-clad silica fiber lasers,” *IEEE J. Quant. Electron.*, **37**, 2, 2001, pp. 207-217, doi: 10.1109/3.903070
8. F. Stutzki, F. Jansen, H. J. Otto, C. Jauregui, J. Limpert and A. Tunnermann, “Designing advanced very-large-mode-area fibers for power scaling of fiber-laser systems,” *Optica*, **1**, 4, 2014, pp. 233-242, doi: 10.1364/OPTICA.1.000233.